nature nanotechnology

LETTERS

PUBLISHED ONLINE: 15 AUGUST 2010 | DOI: 10.1038/NNANO.2010.164

An index for characterization of nanomaterials in biological systems

Xin-Rui Xia, Nancy A. Monteiro-Riviere and Jim E. Riviere*

In a physiological environment, nanoparticles selectively absorb proteins to form 'nanoparticle–protein coronas'[1–5], a process governed by molecular interactions between chemical groups on the nanoparticle surfaces and the amino-acid residues of the proteins[6–8]. Here, we propose a biological surface adsorption index to characterize these interactions by quantifying the competitive adsorption of a set of small molecule probes onto the nanoparticles. The adsorption properties of nanomaterials are assumed to be governed by Coulomb forces, London dispersion, hydrogen-bond acidity and basicity, polarizability and lone-pair electrons. Adsorption coefficients of the probe compounds were measured and used to create a set of nanodescriptors representing the contributions and relative strengths of each molecular interaction. The method successfully predicted the adsorption of various small molecules onto carbon nanotubes, and the nanodescriptors were also measured for 12 other nanomaterials. The biological surface adsorption index nanodescriptors can be used to develop pharmacokinetic and safety assessment models for nanomaterials.

The nano–bio interface consists of a nanoparticle surface, a solid–liquid interface and a corona–media interface (Fig. 1). In aqueous biological systems, the nanoparticle surface is dramatically altered by solvation, the adsorption of small molecules and ionic species[6,9]. This forms the solid–liquid interface, which is key to understanding the behaviour of nanoparticles in biological systems[3,6,10], because it determines the colloidal stability of the nanoparticle in aqueous solutions and determines the affinity and selectivity of biomolecules when forming 'nanoparticle–protein coronas'.

The unique characteristics of this solid–liquid interface arise from the large surface area of the nanoparticles, which preferentially adsorb chemicals or biomolecules to reduce their surface energy[11,12]. The adsorption affinity of a nanomaterial to biomolecules is determined by the contributions of multiple adsorption sites on the nanoparticle surfaces in proximity to the amino-acid residues of the proteins, rather than to an individual and discrete adsorption site[3,6]. The biological surface adsorption index (BSAI) approach characterizes the adsorption properties of nanoparticles by quantifying the competitive adsorption of a set of small molecule probes onto the nanoparticles (Fig. 1, upper right) by mimicking the molecular interactions of the nanoparticle with the amino-acid residues of the proteins (Fig. 1, lower right).

The BSAI approach is based on the fundamental forces of molecular interactions in biological processes: Coulomb force (charged particles), London dispersion (hydrophobic interactions), hydrogen-bond acidity and basicity, dipolarity/polarizability and lone-pair electrons[13]. The Coulomb force can be measured by the zeta-potential of charged nanoparticles. The strength parameters of the other four types of molecular interactions are obtained by the proposed BSAI approach. It is hypothesized that the adsorption properties of nanomaterials are governed by the contributions of each type of molecular interaction, which can be detected by a set of probe compounds with diverse physicochemical properties covering the vector spaces of molecular interactions between the nanomaterial and biomolecules. The adsorption coefficients (k) of the probe compounds can be obtained by measuring the quantities of the probe compounds adsorbed on the surfaces of the nanomaterials and the equilibrium concentrations of the probe compounds in the media. The log k values are scaled to a set of known molecular descriptors of the probe compounds by means of multiple linear regressions to provide a set of nanodescriptors representing the contributions from each type of molecular interactions. Several sets of molecular descriptors (empirical or theoretical) developed in quantitative structure–activity relationship (QSAR) studies can be used for the BSAI approach[14]. Here, the solute solvation descriptors developed by Abraham[15] were used to demonstrate the derivation process. The log k values can be scaled to the solute descriptors by means of a linear free energy relationship (LFER):

$$\log k_i = c + rR_i + p\pi_i + a\alpha_i + b\beta_i + vV_i \quad i = 1, 2, 3, \ldots, n \tag{1}$$

where n is the number of probe compounds, [R_i, π_i, α_i, β_i, V_i] are the molecular descriptors of the ith probe compound from an established database (see Methods). R is the excess molar refraction representing the molecular force of lone-pair electrons, π is the effective solute dipolarity and polarizability, α is the effective solute hydrogen-bond acidity, β is the effective solute hydrogen-bond basicity, and V is the McGowan characteristic volume that represents London dispersion. The regression coefficients [r, p, a, b, v] are the nanodescriptors to be derived from the regression analysis, which represent the relative contributions of the four types of molecular interactions of the nanomaterial at the nano–bio interface. c is the regression constant.

Direct support for the BSAI approach lies in the successful use of the octanol–water partition coefficient (log $K_{o/w}$) in correlation with the biological activities of small molecules[16,17]. This measures the contribution of lipophilic interactions in biological processes[18]. However, it is difficult to measure the log $K_{o/w}$ values for nanomaterials, because most nanomaterials form stable suspensions either in the water or oil phase, but not in both. The key thrust of the BSAI approach is to measure a set of log $K_{o/w}$ equivalent parameters for nanomaterials that can be used for quantitative model development. Correlation of the log $K_{o/w}$ values and the adsorption coefficients (log k) of the probe compounds on multiwalled carbon nanotubes (MWCNTs) is shown in Fig. 2a. This reveals that lipophilicity is a significant factor in the adsorption process, with a correlation slope of 0.68 and R^2 of 0.57, but the scattered data points indicate that lipophilicity is not the only significant factor, with

Center for Chemical Toxicology Research and Pharmacokinetics (CCTRP), North Carolina State University, Raleigh, North Carolina, USA.
*e-mail: jim_riviere@ncsu.edu

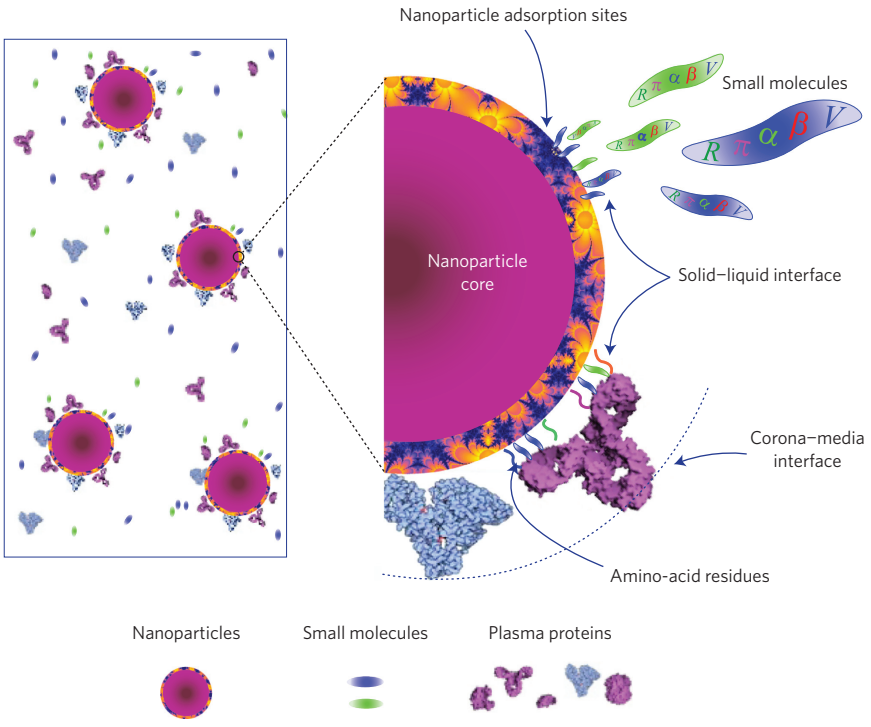

Figure 1 | Illustration of the competitive adsorption of small molecules and proteins onto the surface adsorption sites of nanoparticles. Left: in a physiological environment, nanoparticles are exposed to different proteins and small molecules. Right: the competitive adsorption of small molecules (upper) and the amino-acid residues of proteins (lower) on a nanoparticle. The orange ring on the nanoparticle with blue irregular shapes represents the adsorption sites that are not uniformly distributed on the nanoparticle surface. Small molecules with known molecular descriptors [*R*, *π*, *α*, *β*, *V*] can be used as probes to measure the molecular interaction strengths of the nanoparticles with small molecules and biomolecules.

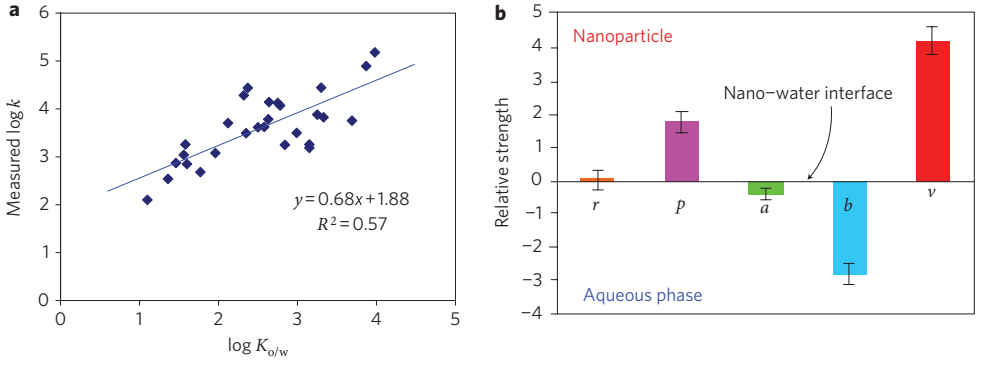

Figure 2 | Relative molecular interaction strengths at the nano–water interface. a, Correlation of the adsorption coefficients (log *k*) of the probe compounds on MWCNTs with their log $K_{o/w}$ values, suggesting that lipophilicity is significant in the adsorption process ($R^2 = 0.57$) but is not the only factor. **b**, The five nanodescriptors [*r*, *p*, *a*, *b*, *v*] measured by the BSAI approach, representing the five major molecular interactions in nanoparticle adsorption processes: lone-pair electrons, polarity/polarizability, hydrogen-bond donor, hydrogen-bond acceptor and London dispersion, respectively. The nanodescriptors of MWCNTs are depicted with standard errors of the regression analysis. Positive values indicate that the nanoparticle surfaces have stronger interaction potentials with the chemicals or biomolecules, and negative values indicate the molecular interactions are stronger in the aqueous phase.

other molecular interactions possibly playing an important role in surface adsorption processes. This observation is consistent with the literature[19].

The BSAI approach has been developed to identify and quantify the significant factors that govern the adsorption properties of nanomaterials. In this study, a set of 28 compounds with diverse physicochemical properties were used as probe compounds. The adsorption coefficients of the probe compounds on a given nanomaterial (for example, MWCNTs) were measured using a solid-phase microextraction (SPME)–gas chromatography mass spectrometry (GC–MS) method. The log *k* values of the probe compounds on MWCNTs and their solvation descriptors [*R*, *π*, *α*, *β*, *V*] are given in Supplementary Table S1. The correlation of log *k* with the solute descriptors was established by means of multiple linear regression analysis of the [log *k*, *R*, *π*, *α*, *β*, *V*] matrix:

$$\log k = -1.33 + 0.043R + 1.75\pi - 0.37\alpha - 2.78\beta + 4.18V \quad (2)$$

where $n = 28$, $R^2 = 0.93$, $F = 63$, $Q^2_{LOO} = 0.888$ and $Q^2_{LMO25\%} = 0.883$.

The nanodescriptors of MWCNTs representing the relative contributions of the four types of molecular interactions are depicted in Fig. 2b. The lipophilicity ($v = 4.18$) is a strong contributor (equation (2)). This is consistent with the result obtained when the

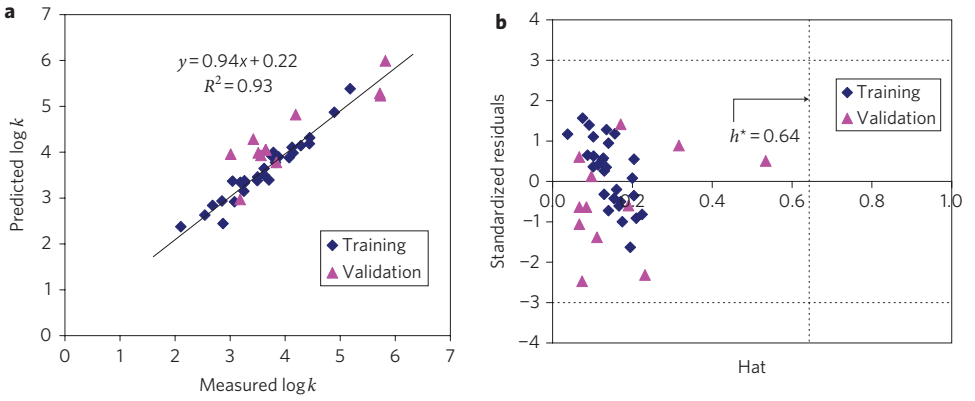

Figure 3 | Predictive model performance and validation for MWCNTs. a, Predicted versus measured log *k* values of the training probe and validation compounds. The predicted log *k* values correlate well ($R^2 = 0.93$) with the measured values of the training probe compounds. The data points of the validation compounds lying close to the regression line reveal the robustness of the predictive model (equation (2)). **b**, Williams plot for verifying the applicability of equation (2). Twelve new compounds were used to validate the model. Training (blue diamonds) and validation (pink triangles) compounds are within the chemical domain (dotted lines) defined by the training probe compounds ($\pm 3\sigma$ and $h^* = 0.64$), suggesting no outliers and the predictivity of the model is reliable. (For an explanation of σ and h^*, see Methods.).

log *k* values were correlated with the log $K_{o/w}$ values of the probe compounds alone (Fig. 2a). Hydrogen-bond basicity ($b = -2.78$) is the second most significant factor, but has a negative value, which suggests that the sorbent surface has a weaker tendency to donate protons (to the probe compounds) than water at the liquid–solid interface. Hydrogen-bond acidity ($a = -0.37$) has a slightly negative value, indicating that the proton acceptor strength of the sorbent surface is slightly weaker than water. The third strong factor is the dipolarity/polarizability ($p = 1.75$), which is an attribute of the huge π-electron clouds on the carbon nanotubes[3,20]. The lone-pair electrons ($r = 0.043$) appear to have a minimal effect, which could be due to the fact that the lone-pair electrons in MWCNTs are shielded inside the π-electron clouds, resulting in them having little effect on the intermolecular adsorption processes. The BSAI approach not only provides rational interpretations for the molecular interactions, but also provides five quantitative physicochemical parameters characterizing the relative strengths of the molecular interactions of the nanomaterials in the adsorption processes.

A plot of the predicted log *k* values of the five nanodescriptors for MWCNTs versus the measured log *k* values are shown in Fig. 3a. A linear correlation was obtained, with a correlation coefficient (R^2) of 0.93. This demonstrated that the five nanodescriptors [*r, p, a, b, v*] of the BSAI approach provide a much better prediction of the adsorption affinity of MWCNTs than lipophilicity (log $K_{o/w}$) alone (Fig. 2a). The partial regression plots and regression residual plot (see Supplementary Information) indicate that the regression model (equation (2)) describes the experimental data well. The robustness of the model was studied by internal cross-validation using the leave-one-out (LOO) and leave-many-out (LMO25%) techniques[21,22], resulting in validation coefficients Q^2_{LOO} of 0.888 and $Q^2_{LMO25\%}$ of 0.883, respectively (see Methods). Both of the cross-validation coefficients were greater than 0.7, revealing the robustness of the predictive model (equation (2))[21].

External validation was conducted using 12 different compounds (measured log *k* values and solute descriptors are given in Supplementary Table S2). The external validation coefficient (Q^2_{ext}) of the model (equation (2)) was 0.78, suggesting satisfactory predictivity for the external validation compounds[21,23]. The applicability domain of the model (equation (2)) was verified using a Williams plot (Fig. 3b). All the training probe and validation compounds are within the chemical domain defined by the training probe compounds ($\pm 3\sigma$ and $h^* = 0.64$), suggesting no outliers, and the predictivity of the model is reliable.

The adsorption of chemicals or biomolecules onto the surface of nanoparticles involves complex processes. In particular, the concentrations of the probe compounds (as a result of multiple layer adsorptions) could affect the values of the adsorption coefficients. Minimum concentrations of the probe compounds should be used in the adsorption experiments to reduce these concentration effects. An operational approach is to measure the nanodescriptors for a given nanomaterial at serial concentrations and then extrapolate to infinitely low concentration to obtain a set of theoretical

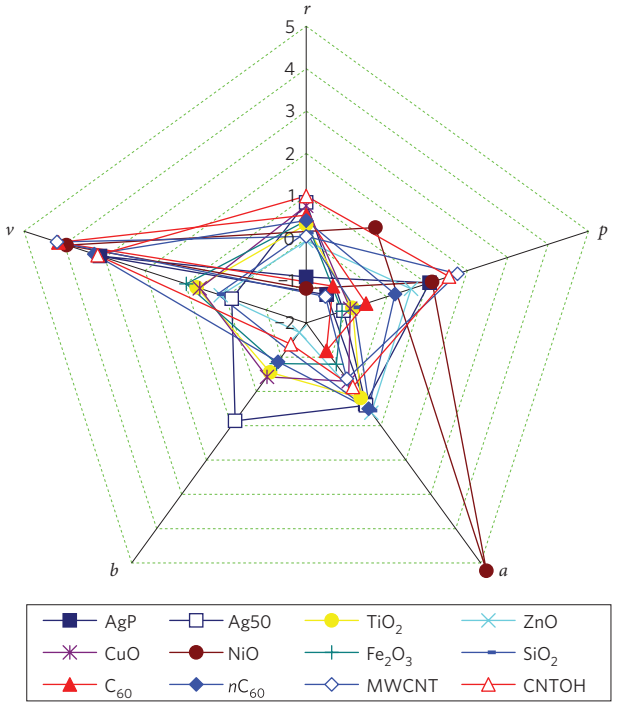

Figure 4 | Radar compass plot comparing the five nanodescriptors of 12 different nanomaterials. The nanodescriptors [*r, p, a, b, v*] are regression coefficients representing the relative molecular interaction strengths of the nanomaterials. The nanodescriptors of NiO nanoparticles showed an irregular pattern because of its unique chemisorption of phenol-derivative probe compounds.

nanodescriptors in an ideal solution[24]. The profiles of the MWCNT nanodescriptors versus concentrations are given in Supplementary Fig. S3. The extrapolated values of the five nanodescriptors [*r, p, a, b, v*] for MWCNTs are 0.21, 1.17, −0.69, −3.24 and 4.31, respectively. The theoretical nanodescriptors would be more generally applicable for the development of predictive models without the concentration effects.

The feasibility of the BSAI approach and some applications of nanodescriptors have been described using MWCNTs as an example. Predictions such as those made for MWCNTs can also be made for other nanomaterials if their five nanodescriptors are measured using the BSAI approach. The BSAI nanodescriptors for 12 additional nanomaterials including silver (AgP: powder and Ag50: colloid), TiO_2, ZnO, CuO, NiO, Fe_2O_3, SiO_2, C_{60} (powder), nC_{60} (colloid), MWCNTs and hydroxylated MWCNTs (CNTOH) were measured. A radar compass plot was used to depict the five nanodescriptors obtained for each of the nanomaterials (Fig. 4). The nanodescriptors of a given nanomaterial provide a signature for comparing its physical chemical properties with other nanomaterials. The nanodescriptors of NiO nanoparticles showed an irregular pattern because of its specific chemisorption of phenol derivatives, suggesting that compounds having specific interactions with a given nanomaterial should not be used as probe compounds for that nanomaterial. In turn, the BSAI approach can be used to identify specific interactions of chemicals or biomolecules that would act as outliers in the predictive model.

One direct application of the BSAI nanodescriptors is to predict the adsorption of small molecules onto nanoparticles, which is a critical process for nanomaterials in biological and environmental systems. Although there are limited quantitative data available in the literature, a few examples are given here as a demonstration. The measured affinity coefficients (log K_f) of polycyclic aromatic hydrocarbons onto MWCNTs[25] correlated well with the predicted log *k* values using the BSAI model (equation (2)), with an R^2 value of 1.00. Correlation of the log K_f values of synthetic organic compounds onto single-walled carbon nanotubes (CNT)[26] with the predicted log *k* values provided an R^2 of 0.86 (Supplementary Figs S4,S5). The predicted log *k* value for a given compound was obtained by inputting the solute descriptors of the compound into the predictive model (equation (2)) (Supplementary Table S3). The predicted interaction strengths of CNTs with the four DNA bases were in the following order: adenine > thymine > guanine > cytosine (Supplementary Fig. S6). This finding may help to interpret conflicting reports in the literature[27].

Steroid hormones are crucial molecules that regulate biological processes and functions in the mammalian body. There are few data on the molecular interactions of hormones with nanomaterials or nanomedicines. When the BSAI model (equation (2)) is used to predict the molecular interaction strengths between MWCNTs and hormones, the log *k* values of testosterone, progesterone, oestradiol, hydrocortisone, aldosterone, L-thyroxine and ethinyl oestradiol were found to be 9.75, 11.2, 9.02, 10.0, 10.7, 12.6 and 9.85, respectively (Table 1). This prediction suggests very strong interactions between MWCNTs and these important hormones, with progesterone in particular being more than one order of magnitude higher than testosterone.

The molecular interactions of a nanomaterial with chemicals and biomolecules are characterized by the BSAI nanodescriptors of the nanomaterial, which also govern the adsorption affinity and selectivity of biomolecules onto the surfaces of the nanomaterial in the corona-formation processes[6–8]. The BSAI nanodescriptors can therefore be used to correlate with the membrane interaction and biodistribution parameters[28] (such as absorption rate, distribution coefficient and extent of cellular uptake) of the nanomaterial to develop physiologically based pharmacokinetic models for the nanomaterial. Similarly, cellular uptake is often a function of protein carriers, so it is crucial to know which proteins a nanoparticle interacts with. The BSAI approach could open a quantitative avenue towards the development of predictive nanomedicine, particularly in the creation of integrated pharmacokinetic models[29] that predict the pathway of cellular uptake[30], and for quantitative risk assessment and safety evaluation of nanomaterials.

Table 1 | Predicted log *k* values of steroid hormones on MWCNTs.

Hormone	*R*	π	α	β	*V*	Predicted log *k*
Testosterone	1.55	2.27	0.31	1.01	2.383	9.75
Progesterone	1.56	2.49	0	1.04	2.622	11.2
Oestradiol	1.85	2.3	0.81	0.95	2.199	9.02
Hydrocortisone	2.04	2.92	0.73	1.9	2.798	10.0
Aldosterone	2.13	3.35	0.48	1.91	2.755	10.7
L-thyroxin	4.14	2.83	1.03	1.31	3.071	12.6
Ethinyl oestradiol	2.07	2.43	0.9	1.02	2.395	9.85

The molecular descriptors [*R*, π, α, β, *V*] were obtained from the Absolv program in the ADME Suite software. The predicted log *k* value for a given hormone was calculated by inputting its molecular descriptor values into the predictive model (equation (2)) for MWCNTs.

Methods

We have developed a SPME/GC–MS method to measure probe compound adsorption onto nanoparticles from aqueous solutions (see Supplementary Information). The SPME method has high analytical sensitivity, measuring the free concentrations of the probe compounds in solution without disturbing the adsorption equilibrium, and without requiring separation of the nanoparticles from the solution, which is the most difficult step in nanoparticle adsorption of small molecules. The GC–MS method offers a high separation power, allowing hundreds of chemicals to be chromatographically separated and quantitated simultaneously[31], which is particularly useful in mimicking the competitive adsorption of biomolecules. The robotic automatic sample analysis enables high-throughput generation of the quantitative data.

The adsorption experiments were conducted by mixing a given quantity of nanomaterial (for example, 2.00 mg MWCNT) with a standard solution containing the probe compounds. The concentration of probe compounds should be minimal although large enough to be quantified accurately in order to reduce the concentration effects among the probe compounds. Only 'parts per billion' levels of the probe compounds (individual concentrations) were required in this study because of the high analytical sensitivity of the SPME/GC–MS method. The ×1 concentrations of the probe compounds are listed in Supplementary Table S1. A number of the commercially available SPME fibres were tested, with polydimethylsiloxane/divinylbenzene (PDMS/DVB) fibres showing optimal performance for quantitative analysis of the probe compounds. After achieving adsorption equilibrium (established from kinetic adsorption experiments, Supplementary Fig. S7), the equilibrium concentration (C_e) of the probe compounds in solution were measured by the SPME/GC–MS method.

The amounts (n^e) of the probe compounds adsorbed by the nanoparticles were obtained by subtracting the quantities remaining in the solution from the dosed amounts in the standard solution ($n^e = V_oC_o - V_oC_e$), where C_o is the standard concentration of a probe compound and V_o is the volume. The surface concentration (C_{ad}) of the probe compound adsorbed on the nanoparticle surfaces was calculated from the adsorption amount (n^e) and the mass (m) of the nanomaterial in the testing solution ($C_{ad} = n^e/m$). The adsorption constant (k) of a given probe compound is the ratio of the surface concentration (C_{ad}) and the equilibrium concentration (C_e) in the solution:

$$k = \frac{C_{ad}}{C_e} = \frac{V_0(C_0 - C_e)}{mC_e} \quad (3)$$

The nanodescriptors for a given nanomaterial were obtained by multiple linear regression analysis of the [log *k*, *R*, π, α, β, *V*] matrix using equation (1). The log *k* values were measured by the adsorption experiments, and the solute descriptors were provided by the Absolv program in the ADME Suite software (Advanced Chemistry Development). An example of the [log *k*, *R*, π, α, β, *V*] matrix for MWCNTs is given in Supplementary Table S1. The regression analysis was performed using the Analyst program in SAS software (SAS Institute).

The robustness of the model (equation (2)) was examined by internal cross-validation using the LOO and LMO25% techniques. $Q^2_{LMO25\%}$ is a stronger cross-validation coefficient than Q^2_{LOO} (ref. 21). The applicability domain of the predictive models was verified by the leverage approach using a Williams plot, with the leverages of the chemicals (diagonal elements of the Hat matrix) versus the Euclidean distances of the compounds to the models measured by the jack-knifed

(standardized and cross-validated) residuals[21,23]. If the jack-knifed residual of a compound is greater than three standard deviation units ($\pm 3\sigma$), the compound will be treated as outliers. If the leverage of the compound is greater than the warning leverage ($h > h^*$), it suggests that the compound is very influential on the model. The warning leverage is defined as $h^* = 3(N+1)/n$, where N is the number of independent variables in the predictive model ($N = 5$ in equation (2)) and n is the number of probe compounds ($n = 28$ in this study).

The external validation of the predictive model (equation (2)) was performed using 12 different compounds. The adsorption coefficients (k) of the 12 validation compounds were measured using the same experimental protocols as described for the training probe compounds. The measured log k values and solute descriptors of the validation compounds are given in Supplementary Table S2. The predicted log k values using equation (2) for the 12 validation compounds are also listed in the table. The external validation coefficient (Q^2_{ext}) was obtained from the measured and predicted log k values of the training probe and validation compounds (Supplementary Tables S1,S2) to verify the predictivity of the regression models[23]:

$$Q^2_{ext} = 1 - \frac{\sum_{i=1}^{i=12}(y_i - \hat{y}_i)^2}{\sum_{i=1}^{i=12}(y_i - \bar{y}_{tr})^2} \quad (4)$$

where y_i and $\hat{y}_i$ are measured log k values and the predicted log k values given by equation (2) of the 12 external validation compounds, and $\bar{y}_{tr}$ is the averaged value of the measured log k values of the training probe compounds (the summations cover all 12 validation compounds).

Received 26 April 2010; accepted 13 July 2010; published online 15 August 2010

References

1. Lynch, I., Dawson, K. A. & Linse, S. Detecting cryptic epitopes created by nanoparticles. *Sci. STKE* **327,** 14 (2006).
2. Cedervall, T. *et al.* Understanding the nanoparticle–protein corona using methods to quantify exchange rates and affinities of proteins for nanoparticles. *Proc. Natl Acad. Sci. USA* **104,** 2050–2055 (2007).
3. Lynch, I. & Dawson, K. A. Protein–nanoparticle interactions. *Nano Today* **3,** 40–47 (2008).
4. Lundqvist, M. *et al.* Nanoparticle size and surface properties determine the protein corona with possible implications for biological impacts. *Proc. Natl Acad. Sci. USA* **105,** 14265–14270 (2008).
5. Hellstrand, E. *et al.* Complete high-density lipoproteins in nanoparticle corona. *FEBS J.* **276,** 3372–3381 (2009).
6. Nel, A. E. *et al.* Understanding biophysicochemical interactions at the nano–bio interface. *Nature Mater.* **8,** 543–557 (2009).
7. Puzyn, T., Leszczynska, D. & Leszczynski, J. Toward the development of 'Nano-QSARs': advances and challenges. *Small* **5,** 2494–2509 (2009).
8. Aillon, K. L., Xie, Y., El-Gendy, N., Berkland, C. J. & Forrest, M. L. Effects of nanomaterial physicochemical properties on *in vivo* toxicity. *Adv. Drug Deliv. Rev.* **61,** 457–466 (2009).
9. Yang, K. & Xing, B. Adsorption of organic compounds by carbon nanomaterials in aqueous phase: Polanyi theory and its application. *Chem. Rev.* doi: 10.1021/cr100059s (2010).
10. Aggarwal, P., Hall, J. B., McLeland, C. B., Dobrovolskaia, M. A. & McNeil, S. E. Nanoparticle interaction with plasma proteins as it relates to particle biodistribution, biocompatibility and therapeutic efficacy. *Adv. Drug Deliv. Rev.* **61,** 428–437 (2009).
11. Patil, S., Sandberg, A., Heckert, E., Self, W. & Seal, S. Protein adsorption and cellular uptake of cerium oxide nanoparticles as a function of zeta potential. *Biomaterials* **28,** 4600–4607 (2007).
12. Simon, P. & Joner, E. Conceivable interactions of biopersistent nanoparticles with food matrix and living systems following from their physicochemical properties. *J. Food Nutr. Res.* **47,** 51–59 (2008).
13. Stone, A. J. (ed.) *The Theory of Intermolecular Forces* (Oxford Univ. Press, 1996).
14. Karelson, M. (ed.) *Molecular Descriptors in QSAR/QSPR* (John Wiley & Sons, 2000).
15. Abraham, M. H. Scales of solute hydrogen-bonding: their construction and application to physicochemical and biochemical processes. *Chem. Soc. Rev.* **22,** 73–83 (1993).
16. Hansch, C. & Fujita, T. A method for the correlation of biological activity and chemical structure. *J. Am. Chem. Soc.* **86,** 1616–1626 (1964).
17. Hansch, C. Quantitative structure—activity relationships and the unnamed science. *Acc. Chem. Res.* **26,** 147–153 (1993).
18. Giaginis, C. & Tsantili-Kakoulidou, A. Alternative measures of lipophilicity: from octanol–water partitioning to IAM retention. *J. Pharm. Sci.* **97,** 2984–3004 (2008).
19. Chen, W., Duan, L. & Zhu, D. Adsorption of polar and nonpolar organic chemicals to carbon nanotubes. *Environ. Sci. Technol.* **41,** 8295–8300 (2007).
20. Arkin, M. R. *et al.* Rates of DNA-mediated electron transfer between metallointercalators. *Science* **273,** 475–480 (1996).
21. Gramatica, P. Principles of QSAR models validation: internal and external. *QSAR Comb. Sci.* **26,** 694–701 (2007).
22. Dearden, J. C., Cronin, M. T. D. & Kaiser, K. L. E. How not to develop a quantitative structure–activity or structure–property relationship (QSAR/QSPR). *SAR QSAR Environ. Res.* **20,** 241–266 (2009).
23. Gramatica, P., Giani, E. & Papa, E. Statistical external validation and consensus modeling: a QSPR case study for K_{oc} prediction. *J. Mol. Graph. Model.* **25,** 755–766 (2007).
24. Duong, D. D. (ed.) *Adsorption Analysis: Equilibria and Kinetics* (Imperial College Press, 1998).
25. Yang, K., Wang, X., Zhu, L. & Xing, B. Competitive sorption of pyrene, phenanthrene and naphthalene on multiwalled carbon nanotubes. *Environ. Sci. Technol.* **40,** 5804–5810 (2006).
26. Zhang, S., Shado, T., Bekaroglu, S. S. & Karanfil, T. The impacts of aggregation and surface chemistry of carbon nanotubes on the adsorption of synthetic organic compounds. *Environ. Sci. Technol.* **43,** 5719–5725 (2009).
27. Johnson, R. R., Johnson, A. T. & Klein, M. L. The nature of DNA-base—carbon-nanotube interactions. *Small* **6,** 31–34 (2010).
28. Xia, X. R., Baynes, R. E., Monteiro-Riviere, N. A. & Riviere, J. E. A system coefficient approach for quantitative assessment of the solvent effects on membrane absorption from chemical mixtures. *SAR QSAR Environ. Res.* **18,** 579–593 (2007).
29. Lee, H. A., Leavens, T. L., Mason, S. E., Monteiro-Riviere, N. A. & Riviere, J. E. Comparison of quantum dot biodistribution with a blood-flow-limited physiologically based pharmacokinetic model. *Nano Lett.* **9,** 794–799 (2009).
30. Zhang, L. W. & Monteiro-Riviere, N. A. Mechanisms of quantum dot nanoparticle cellular uptake. *Toxicol. Sci.* **110,** 138–155 (2009).
31. Xia, X. R. *et al.* A novel *in vitro* technique for studying percutaneous permeation with a membrane-coated fiber and gas chromatography/mass spectrometry Part I. Performances of the technique and determination of the permeation rates and partition coefficients of chemical mixtures. *Pharm. Res.* **20,** 272–279 (2003).

Acknowledgements

This research was supported by the USEPA STAR grant no. R833328 and the United States Air Force Office of Scientific Research (USAFOSR) grant no. FA9550-08-1-0182. The authors thank J. Brooks for help in QSAR validation techniques.

Author contributions

X.-R.X. conceived, conducted and designed the experiments and analysed the resulting data. N.A.M.-R. initiated the application of this technique to nanomaterial characterization and provided biological context. J.E.R. conceived the BSAI concept and contributed to data analysis and interpretation. All three authors were involved in writing and revising the manuscript.

Additional information

The authors declare no competing financial interests. Supplementary information accompanies this paper at www.nature.com/naturenanotechnology. Reprints and permission information is available online at http://npg.nature.com/reprintsandpermissions/. Correspondence and requests for materials should be addressed to J.E.R.